

Analysis of OPAL Bose-Einstein Correlation at Z^0 -pole by the second conventional formula

Takuya Mizoguchi¹, Seiji Matsumoto², and Minoru Biyajima³

¹National Institute of Technology, Toba College, Toba 517-8501, Japan

²School of General Education, Shinshu University, Matsumoto 390-8621, Japan

³Department of Physics, Shinshu University, Matsumoto 390-8621, Japan

July 11, 2022

Abstract

We can obtain a second conventional formula (CF_{II}) with two components by extending the conventional formula CF_I with one component for Bose-Einstein Correlation (BEC). We used CF_{II} to analyze the BEC at Z^0 -pole as part of the OPAL collaboration. $R_1(G) = 0.91 \pm 0.03$ fm ($\lambda_1 = 0.61 \pm 0.03$) and $R_2(G) = 2.57 \pm 0.44$ fm ($\lambda_1 = 0.35 \pm 0.09$) are the estimated interaction region, where λ_1 and λ_2 are the degrees of coherence, and G is the Gaussian distribution, respectively. Long range correlation (LRC) is also studied.

1 Introduction

In the analysis of Bose-Einstein Correlation (BEC) [1–3], the following conventional formula is commonly used,

$$CF_I \cdot LRC = [1.0 + \lambda E_{BE}(R, Q)] \cdot LRC, \quad (1)$$

where E_{BE} is the exchange function between two identical charged pions, which is expressed by

$$E_{BE} = \begin{cases} \exp(-(RQ)^2) & \text{(Gaussian distribution (G))}, \\ \text{or } \exp(-RQ) & \text{(Exponential function (E))}, \end{cases} \quad (2)$$

λ is the degree of coherence. $Q = \sqrt{(p_1 - p_2)^2} = \sqrt{(\mathbf{p}_1 - \mathbf{p}_2)^2 - (E_1 - E_2)^2}$ is the four momentum transfer squared between two identical pions momenta. LRC is the long range correlation, which is typically expressed by

$$LRC = \begin{cases} 1.0 + \delta Q, \\ \text{or } 1.0 + \delta Q + \varepsilon Q^2. \end{cases} \quad (3)$$

The OPAL collaboration used $CF_I(G) \times LRC$ [2] to analyze their data. The results are shown in Table 1 and Fig. 1.

Table 1: Analysis of OPAL data using Eqs. (1)–(3). (G) denotes the Gaussian distribution. $p(\%)$ denotes the p -value in the statistics.

LRC	R (fm)	λ	C	δ (GeV $^{-1}$)	ε (GeV $^{-2}$)
(δ)	1.115 ± 0.026 (G)	0.782 ± 0.039	0.729 ± 0.004	0.162 ± 0.004	—
	$\chi^2/\text{ndf} = 263.8/62$ ($p(\%) = 0.0$)				
(δ, ε)	0.949 ± 0.024 (G)	0.876 ± 0.037	0.630 ± 0.010	0.489 ± 0.034	-0.126 ± 0.012
	$\chi^2/\text{ndf} = 113.9/61$ ($p(\%) = 0.0046$)				

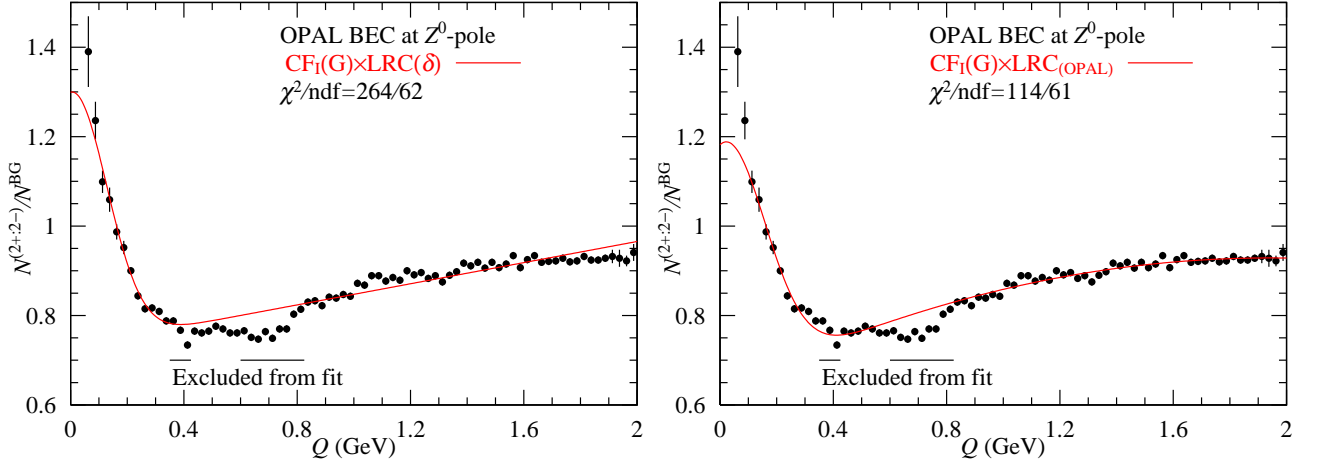


Figure 1: Analysis of the OPAL BEC at the Z^0 -pole by Eq. (1) with Eqs. (2) and (3).

In Refs. [4–8], we analyzed the BEC at 0.9 TeV and 7 TeV by CMS collaboration using the CF_I formula. In those analyses, χ^2/ndf 's are very large. To improve them, we use the CF_II formula, which corresponds to the nondiffractive and diffractive process in pp collisions with two components,

$$\text{CF}_\text{II} \cdot \text{LRC} = [(1.0 + \lambda_1 E_{\text{BE}_1}(R_1, Q) + \lambda_2 E_{\text{BE}_2}(R_2, Q))] \cdot \text{LRC}_{(\text{OPAL})}. \quad (4)$$

Indeed, χ^2/ndf 's became smaller values. Thus, we expect that Eq. (4) also works for the BEC at Z^0 -pole because there are two types of events in e^+e^- annihilation. See Fig. 2 [9–12].

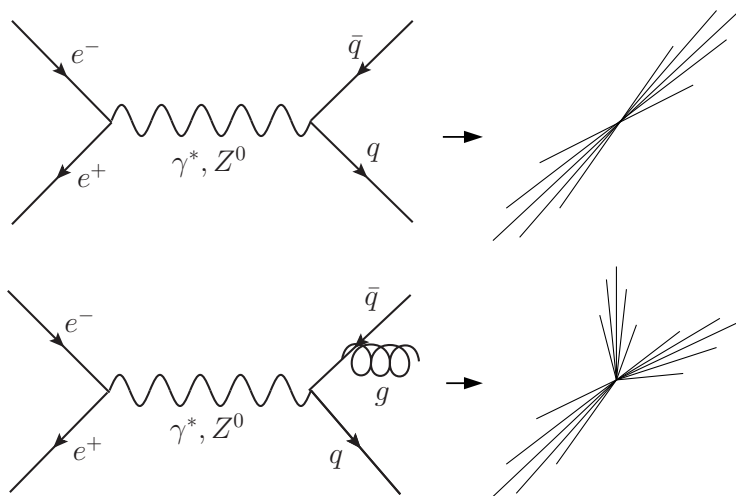


Figure 2: Jet-production in e^+e^- annihilation.

In section 2, we analyze the BEC at Z^0 -pole by $\text{CF}_{\text{II}} \times \text{LRC}_{(\text{OPAL})}$, because there are the 2-jet and 3-jet events in e^+e^- collisions at Z^0 -pole. In section 3, we investigate the $\text{LRC}_{(\text{OPAL})}$ from a slightly different angle, considering the behavior in the large and small Q regions. In section 4, the profile of LRC's and the exchange functions in the Euclidean space is studied. In the final section, we present the concluding remarks.

2 Analysis of BEC using $\text{CF}_{\text{II}} \times \text{LRC}_{(\text{OPAL})}$

First, we focus on the results in Table 1. Because they are considered the first approximation, we adopt the following constraints for R_1 , λ_1 , c , δ , and ε :

$$q - \sigma_q \leq q \leq q + \sigma_q \Rightarrow \begin{cases} 0.925 \leq R_1 \leq 0.973 \text{ (fm)}, \\ 0.840 \leq \lambda_1 \leq 0.914, \\ 0.620 \leq C \leq 0.640, \\ 0.455 \leq \delta \leq 0.523 \text{ (GeV}^{-1}\text{)}, \\ -0.138 \leq \varepsilon \leq -0.114 \text{ (GeV}^{-2}\text{)}. \end{cases} \quad (5)$$

Moreover, the following three constraints are introduced (Fig. 2).

$$\lambda_2 < \lambda_1, \quad \lambda_1 + \lambda_2 \leq 1.0, \quad \text{and} \quad R_1 < R_2. \quad (6)$$

In Fig. 2, R_2 and λ_2 denote the interaction region and the second degree of coherent of 3-jet, respectively.

$\text{CF}_{\text{II}}(\lambda_1 G_1 + \lambda_2 G_2)$ and $\text{CF}_{\text{II}}(\lambda_1 G_1 + \lambda_2 E_2)$ are two plausible geometrical combinations. Among them, the $\text{CF}_{\text{II}}(\lambda_1 G_1 + \lambda_2 G_2)$ has the minimum χ^2/ndf . Thus, our result by $\text{CF}_{\text{II}}(\lambda_1 G_1 + \lambda_2 G_2) \cdot \text{LRC}_{(\text{OPAL})}$ is shown in Tables 2 and 3, as well as Fig. 3.

Table 2: Estimated parameters using Eq. (4) with the geometrical combination $(\lambda_1 G_1 + \lambda_2 G_2)$ and the constraint $\lambda_1 + \lambda_2 \leq 1.0$.

R_1 (fm) (G)	R_2 (fm) (G)	λ_1	λ_2
0.925 ± 0.048	1.926 ± 0.277	0.840 ± 0.050	0.160 ± 0.024
C	δ (GeV $^{-1}$)	ε (GeV $^{-2}$)	χ^2/ndf ($p(\%)$)
0.624 ± 0.004	0.509 ± 0.017	-0.133 ± 0.007	$104.9/59$ (0.022)

Table 3: Estimated parameters using Eq. (4) with the geometrical combination $(\lambda_1 G_1 + \lambda_2 G_2)$. Although $\lambda_1 + \lambda_2$ is not bounded, the assumption $\lambda_1 + \lambda'_2 = 1.0$ is used. Δ denotes the difference between the dot-dot line and solid line in Fig. 3. The OPAL collaboration observed that $\Delta = 0.15$ [2].

R_1 (fm) (G)	R_2 (fm) (G)	λ_1	λ_2
0.931 ± 0.009	2.506 ± 0.339	0.841 ± 0.010	0.521 ± 0.159
C	δ (GeV $^{-1}$)	ε (GeV $^{-2}$)	χ^2/ndf ($p(\%)$)
0.626 ± 0.006	0.501 ± 0.021	-0.130 ± 0.008	$98.7/59$ (0.091)
Note	R_2 (fm)	λ'_2	λ''_2
“ $\lambda_1 + \lambda'_2 = 1.0$ ” is assumed.	2.51 ± 0.34	0.16 ± 0.01	0.36 ± 0.16
		2nd-BEC from 3-jet.	Contribution from η' and η decay chain, $\Delta \cong 0.13$.

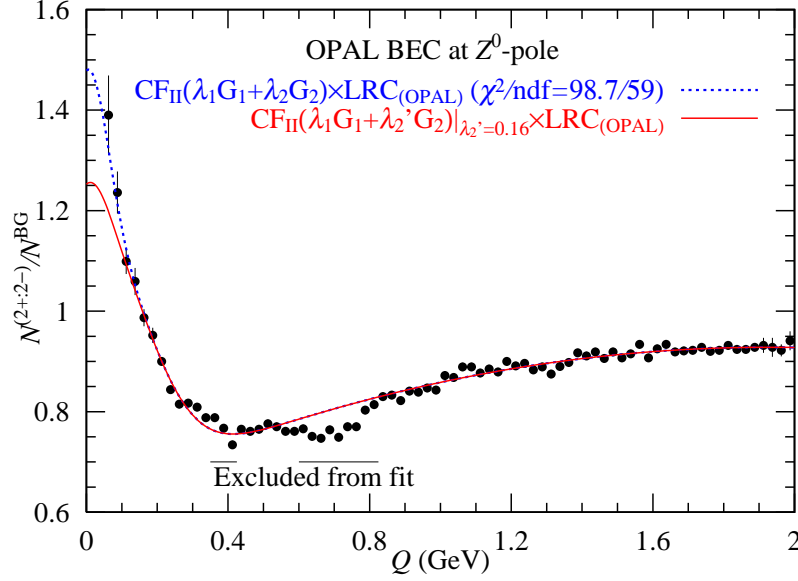


Figure 3: Analysis of the OPAL BEC at the Z^0 -pole by Eq. (4) with no-constraint for λ_1 and λ_2 . $LRC_{(OPAL)} = 1.0 + \delta Q + \varepsilon Q^2$. See Table 3.

3 Different expressions of $LRC_{(OPAL)}$

3.1 Inclusion of higher order of variable Q in LRC

Fig. 4 shows the behavior of $LRC_{(OPAL)}$. We observe that $LRC_{(OPAL)}$ becomes $C = 0.63$ at $Q \cong 4$ GeV. Indeed that behavior is a parabolic curve.

Here, we introduce a function $X = \alpha Q e^{-\beta Q} = \alpha Q (1 - \beta Q + \beta^2 Q^2 / 2! - \dots)$ and it is a power series because α and β are two parameters, as shown below.

$$\begin{aligned} LRC_{(p.s.)} &= C \left[\sum_{k=0}^{\infty} (\alpha Q e^{-\beta Q})^k \right], \\ &= \frac{C}{1 - \alpha Q e^{-\beta Q}}. \end{aligned} \quad (7)$$

In Eq. (7), we can avoid the following behavior in $LRC_{(OPAL)}$ (in the region $Q > 4.0$ GeV),

$$LRC_{(OPAL)} \xrightarrow{Q \rightarrow \text{large}} \text{negative values.}$$

Fig. 4 compares two LRCs, $LRC_{(OPAL)}$ and $LRC_{(p.s.)}$. The Fig. coincidence between $LRC_{(OPAL)}$ and $LRC_{(p.s.)}$ in the region $Q \leq 2.0$ GeV seems to be excellent. Moreover, $LRC_{(p.s.)}$ gradually becomes the constant values C at large Q .

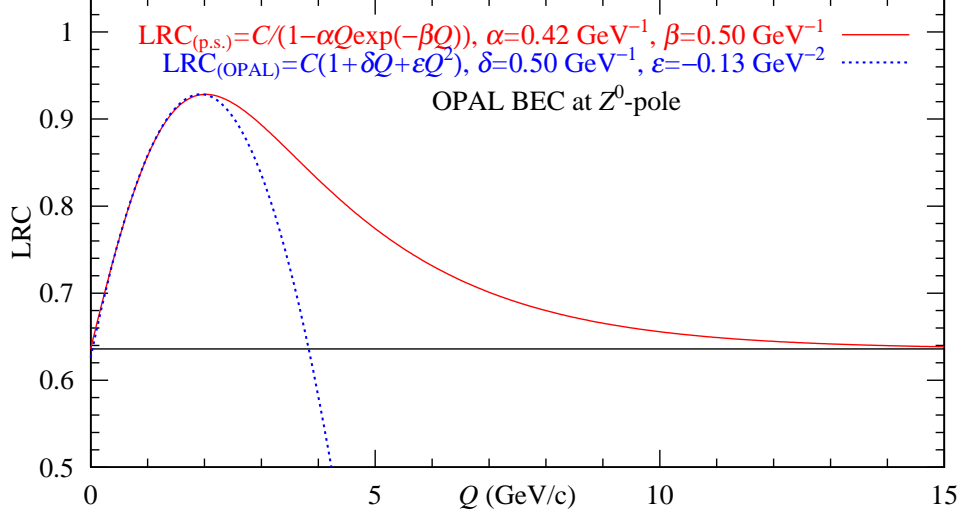


Figure 4: LRCs of the OPAL BEC at the Z^0 -pole by Eqs. (4) and (8). Numerical values are presented in Tables 3 and 4.

This time the following formula is used in our analysis.

$$\text{CF}_{\text{II}} \times \text{LRC}_{(\text{p.s.})} = (1.0 + \lambda_1 E_{\text{BE}_1}(R_1, Q) + \lambda_2 E_{\text{BE}_2}(R_2, Q)) \cdot \text{LRC}_{(\text{p.s.})} \quad (8)$$

Our result from Eq. (8) is presented in Fig. 5 and Table 4, and it is almost the same as those shown in Table 3.

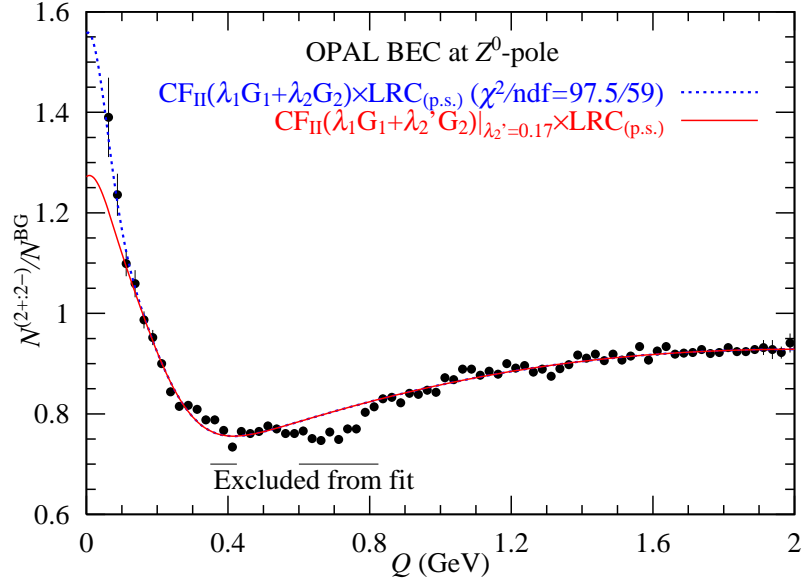


Figure 5: Analysis of the OPAL BEC at the Z^0 -pole by Eq. (8). $\text{LRC}_{(\text{p.s.})} = \sum_{k=0}^{\infty} (\alpha Q e^{-\beta Q})^k$. See Table 4.

Table 4: Estimated parameters using Eq. (8) with the geometrical combination ($\lambda_1 \times G_1 + \lambda_2 \times G_2$). Although $\lambda_1 + \lambda_2$ is not bounded, the assumption $\lambda_1 + \lambda'_2 = 1.0$ is used. Δ denotes the difference between the dot-dot line and solid line in Fig. 5. The OPAL collaboration observed that $\Delta = 0.15$ [2].

R_1 (fm) (G)	R_2 (fm) (G)	λ_1	λ_2
0.930 ± 0.010	2.659 ± 0.361	0.826 ± 0.008	0.623 ± 0.205
C	α (GeV $^{-1}$)	β (GeV $^{-1}$)	χ^2/ndf ($p(\%)$)
0.636 ± 0.005	0.424 ± 0.016	0.495 ± 0.014	$97.5/59$ (0.12)
Note	R_2 (fm)	λ'_2	λ''_2
“ $\lambda_1 + \lambda'_2 = 1.0$ ” is assumed.	2.66 ± 0.36	0.17 ± 0.01	0.45 ± 0.21
		2nd-BEC from 3-jet.	Contribution from η' and η decay chain, $\Delta \cong 0.15$.

3.2 Separation of η' and η decay chain using a modification of $\text{LRC}_{(\text{p.s.})}$

In a previous subsection, we included the resonance effect due to η' and η decay chain into CF_{II} without the constraint $\lambda_1 + \lambda_2 \leq 1.0$. Hereafter, we include the resonance effect in the LRC as follows.

The power series in Eq. (7) is $\sum_{k=1}^{\infty} X^k$, which is an increasing function in the region $Q \leq 2.0$ GeV. Here we adopt the following alternating series $\text{LRC}_{(\text{a.p.s.})} = \sum_{k=0}^{\infty} (-X)^k = 1.0 - X + X^2 - X^3 + X^4 - X^5 + X^6 - \dots$,

$$\begin{aligned} \text{LRC}_{(\text{a.p.s.})} &= C \left[\sum_{k=0}^{\infty} (-\alpha Q e^{-\beta Q})^k \right] \\ &= \frac{C}{1 + \alpha Q e^{-\beta Q}} \end{aligned} \quad (9)$$

because it is the decreasing function from $Q = 0.0$ GeV and increasing from $Q = 1/\beta$ GeV, implying the local minimum point. Thus, we can expect a possibility in Eq. (9) as a role of an alternative LRC.

$$\text{CF}_{\text{II}} \times \text{LRC}_{(\text{a.p.s.})} = (1.0 + \lambda_1 E_{\text{BE}_1}(R_1, Q) + \lambda_2 E_{\text{BE}_2}(R_2, Q)) \cdot \text{LRC}_{(\text{a.p.s.})} \quad (10)$$

Table 5 and Fig. 6 show our result from Eq. (10). Note that the estimated $\lambda_1 + \lambda_2 = 0.49 + 0.21 = 0.70 < 1.0$ is less than the bind value because $\text{LRC}_{(\text{a.p.s.})}$ (Eq. (9)) absorbed the resonance effect. By using estimated parameters, we can calculate the contributions of 2-jet and 3-jet as follows;

$$\begin{aligned} S_2 &= \text{contribution of 2-jet} = \frac{\lambda_1 \sqrt{\pi}}{2 \times R_1 \times 5.0} = 0.093, \\ S_3 &= \text{contribution of 3-jet} = \frac{\lambda_2 \sqrt{\pi}}{2 \times R_2 \times 5.0} = 0.015. \end{aligned}$$

The ratio of S_3 to all-jet is obtained as follows:

$$R_{3\text{-all-jet}} = \frac{S_3}{S_2 + S_3} = \frac{0.015}{0.108} = 0.14 = 14\%$$

The ratio $R_{3\text{-all-jet}} = 14\%$ is compatible with the emperical value $17.4 \pm 0.7\%$ in Refs. [12, 13].

Table 5: Estimated parameters using Eqs. (9) and (10) with the geometrical combination ($\lambda_1 \times G_1 + \lambda_2 \times G_2$).

R_1 (fm) (G)	R_2 (fm) (G)	λ_1	λ_2
0.895 ± 0.017	2.393 ± 0.512	0.498 ± 0.016	0.223 ± 0.075
C	α (GeV $^{-1}$)	β (GeV $^{-1}$)	χ^2/ndf ($p(\%)$)
0.938 ± 0.002	2.359 ± 0.056	3.254 ± 0.042	$86.3/59$ (1.2)

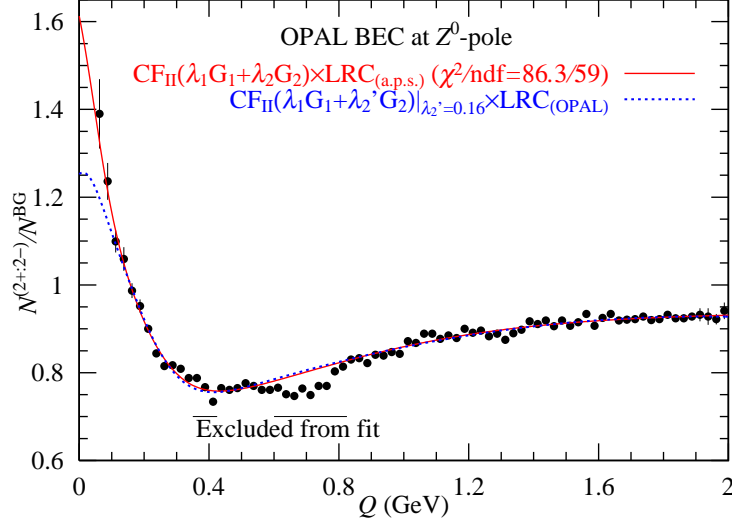


Figure 6: Analysis of the OPAL BEC at the Z^0 -pole by Eq. (10).

In Fig. 7, we compare the two LRC's. The rapidly decreasing behavior of $\text{LRC}_{(a.p.s.)}$ in the region of $0 < Q < 0.3$ GeV could be due to the resonance effect of the η' and η decay chain, but the coincidence of $\text{LRC}_{(OPAL.)}$ and $\text{LRC}_{(a.p.s.)}$ in the region of $0.5 < Q < 2.0$ GeV is remarkable. In this region, $\text{LRC}_{(a.p.s.)}$ plays the role of $\text{LRC}_{(OPAL.)}$.

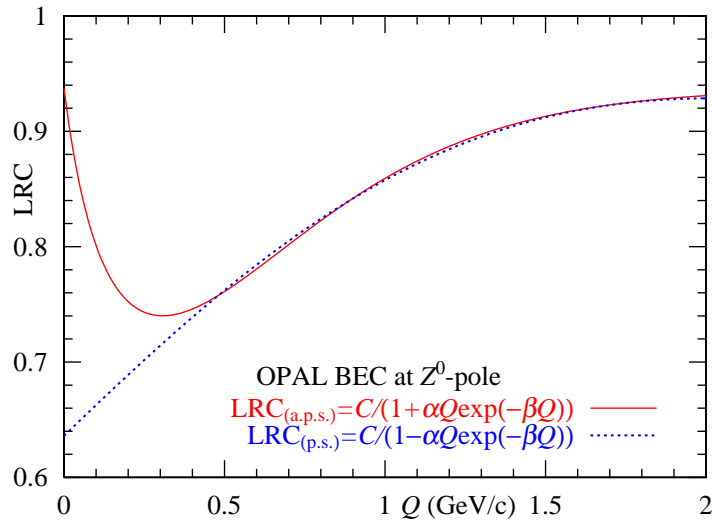


Figure 7: LRCs of the OPAL BEC at the Z^0 -pole by Eq. (8). Numerical values are presented in Tables 4 and 5.

3.3 Estimation of the contamination due to π - K pair through $f(Q) = 0.81 - 0.07Q$ à la OPAL

In conclusion, we corrected for π - K pair the contamination using the OPAL method, i.e., $f(Q) = 0.81 - 0.07Q$ [2, 17]. In Eq. (7), $\lambda_1 f(Q)$ and $\lambda_2 f(Q)$ are used in the analysis. Our results are presented in Table 6. The p -value was improved from 0.98 in Table 5 to 1.34 in Table 6. Moreover, $\lambda_1 + \lambda_2 < 1.0$ is satisfied in Table 6 in this case. From Table 6, we obtain the ratio $R_{3\text{-all-jet}} = 17\%$. This figure probably reflects the correlation of the π - K pair.

Table 6: To account contaminating the π - K pair, we use the OPAL collaboration's function $f(Q) = 0.81 - 0.07Q$. $\lambda_1 f(Q)$ and $\lambda_2 f(Q)$ are used in the analysis.

$\text{CF}_{\text{II}} \times \text{LRC}_{(\text{a.p.s.})}$	R_1 (fm) (G)	R_2 (fm) (G)	λ_1	λ_2
	0.912 ± 0.031	2.574 ± 0.435	0.605 ± 0.026	0.348 ± 0.087
	C	α (GeV^{-1})	β (GeV^{-1})	χ^2/ndf ($p(\%)$)
	0.941 ± 0.002	2.222 ± 0.037	3.139 ± 0.046	$85.6/59$ (1.34)
$\text{CF}_{\text{I}} \times \text{LRC}_{(\text{OPAL})}$	R (fm)	λ		
	0.944 ± 0.024	1.091 ± 0.046		
	C	δ (GeV^{-1})	ε (GeV^{-2})	χ^2/ndf ($p(\%)$)
	0.629 ± 0.010	0.490 ± 0.034	-0.126 ± 0.013	$113.3/59$ (0.0054)

4 Profile of $\text{LRC}_{(\text{a.p.s.})}$ and $(\lambda_1 \mathbf{G}_1 + \lambda_2 \mathbf{G}_2)$ in the Euclidean space

In the previous section, we obtained the concrete values ($\alpha = 2.15 \text{ GeV}^{-1} = 2.15/5.07 \text{ fm}$ and $\beta = 3.08/5.07 \text{ fm}$) in $\text{LRC}_{(\text{a.p.s.})}$. Then, using the following formula [14, 15], we can calculate the profile of $(\text{LRC}_{(\text{p.s.})} - 1.0)$ in the Euclidean space. Its variable is expressed by $\xi = \sqrt{(x_1 - x_2)^2} = \sqrt{(\mathbf{r}_1 - \mathbf{r}_2)^2 + (t_1 - t_2)^2}$ where x_1 and x_2 denote the space-time coordinates of two pions. For the behavior of $(\text{LRC}'_{\text{s}} - 1)$ in the Euclidean space, we have the following density profile of $(\text{LRC} - 1)$ with $s = \pm 1$ [14–16]

$$\begin{aligned}
\rho_{(\text{LRC}-1.0)}(\xi) &= \frac{\xi^2}{2} \int_0^\infty Q^2 \sum_{k=1}^\infty (s)^k (\alpha Q e^{-\beta Q})^k J_1(\xi Q) dQ \\
&= \frac{\xi^2}{2} \sum_{k=1}^\infty (s\alpha)^k \frac{\Gamma(k+2+2)}{((k\beta)^2 + \xi^2)^{(k+2+1)/2}} \text{P}_{k+2}^{-1} \left(\frac{k\beta}{\sqrt{(k\beta)^2 + \xi^2}} \right) \\
&= \frac{\xi^2}{2} \left[(s\alpha) \frac{\Gamma(5)}{(\beta^2 + \xi^2)^2} \text{P}_3^{-1} \left(\frac{\beta}{\sqrt{\beta^2 + \xi^2}} \right) \right. \\
&\quad \left. + (s\alpha)^2 \frac{\Gamma(6)}{((2\beta)^2 + \xi^2)^{2.5}} \text{P}_4^{-1} \left(\frac{2\beta}{\sqrt{(2\beta)^2 + \xi^2}} \right) \right. \\
&\quad \left. + (s\alpha)^3 \frac{\Gamma(7)}{((3\beta)^2 + \xi^2)^3} \text{P}_5^{-1} \left(\frac{3\beta}{\sqrt{(3\beta)^2 + \xi^2}} \right) + \dots \right], \tag{11}
\end{aligned}$$

where P_{k+2}^{-1} is the associate Legendre function and “s” is the sign function defined as follows,

$$\begin{cases} s = +1 & \text{for LRC}_{(p.s)}, \\ s = -1 & \text{for LRC}_{(a.p.s)}. \end{cases}$$

It is noted that Eq. (11) is calculated in the Euclidean space, where the variable $Q_W = \sqrt{(\mathbf{p}_1 - \mathbf{p}_2)^2 + (E_1 - E_2)^2}$ should be used. The index W means the Wick rotation. However, because we have no such physical quantities described by Q_W , we use quantities describe by $Q = \sqrt{(\mathbf{p}_1 - \mathbf{p}_2)^2 - (E_1 - E_2)^2}$ as an approximate calculation. Thus the variable ξ should be regarded as $D = \sqrt{x^2} = \sqrt{(\mathbf{r}_1 - \mathbf{r}_2)^2 - (t_1 - t_2)^2}$ in Fig. 8 using a revised Wick rotation, when it is necessary [18, 19].

Fig. 8 show the density of the profile $\rho_{(\text{LRC}-1.0)}(\xi)$ because $\int_0^\infty Q^2 J_1(\xi Q) dQ$ is divergent. We simultaneously present two Gaussian functions multiplied by the phase space $2\pi^2 \xi^3$;

$$\rho_G(\xi) = \frac{\xi^3}{8R^4} \exp\left(-\frac{\xi^2}{4R^2}\right). \quad (12)$$

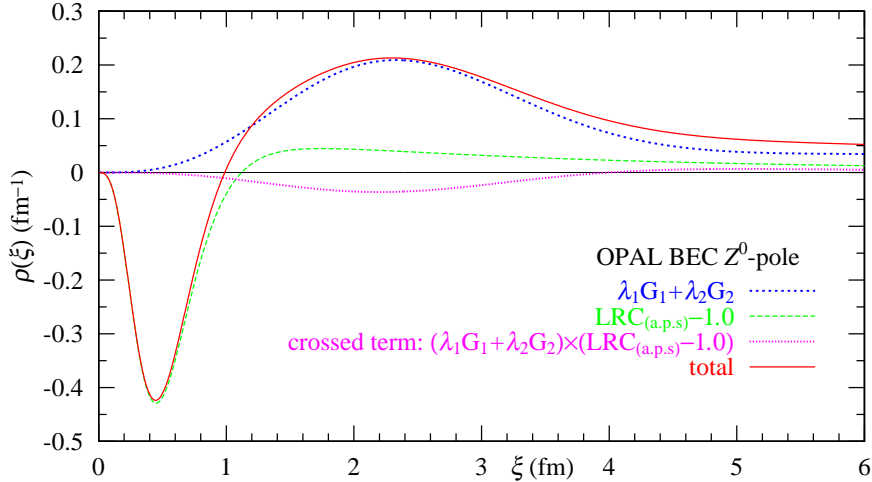


Figure 8: Pion-pairs density distributions of the OPAL BEC at Z^0 -pole in four-dimensional Euclidean space, where ξ denotes the distance between two pion-production points. The contribution of the crossed terms $((\lambda_1 G_1 + \lambda_2 G_2) \times \rho_{(\text{LRC}-1)})$, i.e., the probability is small. The value of $C = 0.942$ from Table 5 is used.

The dip at $\xi = 0.5$ fm is due to the resonance effect of the η' and η decay chain assigned to LRC mentioned in the subsection 3.2. The role of the dip is the contamination at Z^0 -pole in e^+e^- collision. The magnitude of the area of the entire profile is $C(\lambda_1 + \lambda_2) \cong 1.0$. Note that the contribution of $(\text{LRC}_{(p.s.)} - 1.0)$ in the entire region $(0 < \xi < \infty)$ is zero.

5 Concluding remarks

We summarize our present analysis.

C.I: We propose the second conventional formula with two sources in Eq. (4). This formula reflects the physical processes shown in Fig. 2. There are two types of 2-jet and 3-jet events at Z^0 -pole. The CF_{II} has a description option. In concrete analysis, the second contribution described

by the $\lambda_2 \times \text{exchange}$ function E_{BE_2} is treated as the second approximation. To achieve this goal, we used the inequalities mentioned in Eq. (5) in our analysis.

C.II: We propose an analytic formulation for the LRC with $X = \alpha Q e^{-\beta Q} = \alpha Q (1 - \beta Q + \beta^2 Q^2 / 2! - \dots)$, with two parameters, α and β , which are corresponding to parameters δ and ε by OPAL collaboration— [2]. In our analysis, we use the power series, $\text{LRC}_{(\text{p.s.})} = \sum_{k=0}^{\infty} X^k$. In the region $0 \leq Q \leq 2$ GeV, $\text{LRC}_{(\text{p.s.})}$ is almost equivalent with $\text{LRC}_{(\text{OPAL})}$ (Fig. 4).

C.III: We demonstrated that results with the constraint $\lambda_1 + \lambda_2 \leq 1.0$ and $\lambda_1 + \lambda_2 = \text{free}$ in Eq. (4). In the second analysis including the second term with λ_2 , we assume that the separation of λ_2 is possible: $\lambda_2 = \lambda'_2 + \lambda''_2$ and $\lambda'_2 = 1.0 - \lambda_1$. λ'_2 is the second contribution to BEC. The remaining part λ''_2 describes the resonance effect due to the η' and η decay chains. Based on this assumption, we estimate the resonance effect as Δ in the region $Q \leq 0.15 \sim 0.3$ GeV in the note column in Table 4.

C.IV: We separate the resonance effect due to the η' and η decay chain in BEC using $\text{CF}_{\text{II}}(\lambda_1 G_1 + \lambda_2 G_2) \times \text{LRC}_{(\text{p.s.})}$ analysis. We consider the alternation of $\text{LRC}_{(\text{p.s.})}$ to improve this separation. To that end, we propose the following formula $\text{LRC}_{(\text{a.p.s.})}$ in Eq. (9). Our result in terms of Eq. (10) is shown in Table 5. The contributions of the 2-jet event and the 3-jet event are estimated in that analysis. The 3-jet to all-jet $R_{3\text{-all-jet}}$ ratio is approximately $0.14 = 14\%$, which is consistent with the measurement by OPAL collaboration, $R_{3\text{-all-jet}} = 17.4 \pm 0.7 \%$ [12, 13].

C.V: Moreover, we followed the method by OPAL collaboration with $f(Q) = 0.81 - 0.07Q$ [2, 17], to subtract the contamination of π - K pairs,

$$\lambda f(Q) \times \text{Gaussian function} \longrightarrow \lambda_1 f(Q) G_1 + \lambda_2 f(Q) G_2$$

In the analysis, the sum of the degrees of coherence λ_1 and λ_2 , $\lambda_1 + \lambda_2 \approx 0.95 < 1.0$ and the p-value is $p(\%) = 1.34$ is shown in Table 6. We can compare our result with that of $\text{CF}_1 \times \text{LRC}_{(\text{OPAL})}$.

C.VI: Moreover, we investigate the profiles of $(\text{LRC}_{(\text{a.p.s.})} - 1.0)$ and the exchange functions in Fig. 8. The profiles of $(s\alpha Q e^{-\beta Q})^k$ ($k = 1, 2, 3$) are calculated in Eq. (11). There is an interesting property in $\rho_{(\text{a.p.s.})}^{(k)}(\xi)$: The magnitude of the area of $\rho_{(\text{a.p.s.})}^{(k)}(\xi) > 0$ is the same as that of $\rho_{(\text{a.p.s.})}^{(k)}(\xi) < 0$ because of the property of the associate Legendre function. This is remarkable for the physical property of LRCs.

D.I: The OPAL BEC region is restricted to $0.0 < Q < 2.0$ GeV. When the upper limit increased, for example, 4.0 GeV, we can obtain more physical information on LRCs (Fig. 7). The upper value of integration in Eq. (12) is infinity. If we replace it with $Q = 4$ GeV, we obtain almost the same figures in Fig. 8.

D.II: We would like to analyze the other BECs at 0.9 TeV and 7 TeV with CMS collaboration using Eq. (4) in the future.

Acknowledgments. One of authors (M.B.) would like to thank his colleagues at Department of Physics in Shinshu University.

References

- [1] R. Hanbury Brown, and R. Q. Twiss, *Nature*, **177** (1956) 27.
- [2] P. D. Acton *et al.* [OPAL Collaboration], *Phys. Lett. B* **267** (1991) 143.
- [3] P. Abreu *et al.* [DELPHI Collaboration], *Phys. Lett. B* **286** (1992) 201.
- [4] G. Aad *et al.* [ATLAS Collaboration], *Eur. Phys. J. C* **75** (2015) 466.
- [5] V. Khachatryan *et al.* [CMS Collaboration], *JHEP* **1105** (2011) 029.
- [6] M. Biyajima and T. Mizoguchi, *Eur. Phys. J. A* **54** (2018) 105;
 Therein, for N^{BG} , an identical separation between two ensembles with α_1 and α_2 is assumed.
 When there is no separation between them, the following formula is obtained:

$$N^{(2+;2-)} / N^{\text{BG}} = 1 + (a_1/s)(2/k_1)E_1^2 + (a_2/s)(2/k_2)E_2^2,$$
 where $s = a_1 + a_2 = \alpha_1 \langle n_1 \rangle^2 + \alpha_2 \langle n_2 \rangle^2$ (see succeeding Refs. [7, 8]).
- [7] T. Mizoguchi and M. Biyajima, *JPS Conf. Proc.* **26** (2019) 031032.
- [8] M. Biyajima and T. Mizoguchi, *Int. J. Mod. Phys. A* **34** (2019) 1950203.
- [9] T. Mizoguchi and M. Biyajima, *Int. J. Mod. Phys. A* **35** (2020) 2050052.
- [10] A. Giovannini, S. Lupia, and R. Ugoccioni *Phys. Lett. B* **374** (1996) 231.
- [11] B. Foster ed., “Electron-positron annihilation physics” (Adam Hilger; Bristol, 1990).
- [12] D. Duchesneau, J. H. Field, and H. Jeremie, “Quarks and gluons : tests of QCD in e^+e^- annihilations”, *C. R. Acad. Sci. Paris* 3, 9 (2002) 1211.
- [13] Y. Totsuka “Particle Physics” (In Japanese, Iwanami shoten, Tokyo, 1992). See Fig 5-19.
- [14] R. Shimoda, M. Biyajima, and N. Suzuki, *Prog. Theor. Phys.* **89** (1993) 697.
- [15] Ian N. Sneddon, “Fourier Transforms” (Dover Pub., Inc, NY, 1995).
- [16] T. Mizoguchi and M. Biyajima, [arXiv:2102.11083 [hep-ph]].
- [17] S. K. Choi *et al.* [AMY Collaboration], *Phys. Lett. B* **355** (1995) 406.
- [18] S. Tomonaga et al., “Quantum Theory of Fields” (In Japanese, Iwanami shoten, Tokyo, 1955).
- [19] G. A. Kozlov, O. V. Utyuzh, G. Wilk, and Z. Wlodarczyk, *Phys. Atomic Nuclei* **71** (2008) 1502.